



Contribution of Transmembrane Protein 68 to Triglyceride Synthesis and Lipid Droplet Formation Differs From Diacylglycerol Acyltransferase*

YU Qing, FU Yang-Yang, ZENG Fan-Si, PANG Hui-Min, HUANG Fei-Fei, CHANG Ping-An**

(Chongqing Key Laboratory of Big Data for Bio-Intelligence, School of Life Health Information Science and Engineering,

Chongqing University of Posts and Telecommunications, Chongqing 400065, China)

Abstract Objective To characterize transmembrane protein 68 (TMEM68) in an alternative triacylglycerol (TAG) biosynthesis pathway, and determine the interplay between TMEM68 and the canonical TAG synthesis enzyme acyl-CoA: diacylglycerol acyltransferase (DGAT). **Methods** Effects of exogenous fatty acid and monoacylglycerol on TAG synthesis and lipid droplet (LD) formation in TMEM68 overexpression and knockout cells treated with DGAT inhibitor or not were investigated by comparing LD morphology, Oil Red O staining, and measurement of TAG levels. LDs were stained with fluorescence dye and observed by confocal fluorescence microscopy. TAG levels were determined with an enzyme-based triglyceride assay kit. Colocalization of TMEM68 and DGAT1 was detected by co-expression and confocal fluorescence microscopy and their interaction was determined by co-immunoprecipitation. RT-qPCR and immunoblotting assay were used to detect the expression of DGAT1. **Results** The synthesis of TAG catalyzed by TMEM68 was independent of DGAT activity. Surplus exogenous fatty acids and monoacylglycerol promoted TAG synthesis mainly through DGAT in human neuroblastoma cells. The LDs formed by TMEM68 were different in morphology from those by DGAT. In addition, TMEM68 and DGAT1 colocalized in the same endoplasmic reticulum (ER) compartment but did not interact physically. TMEM68 overexpression reduced the expression of DGAT1, the major DGAT enzyme involved in TAG synthesis, while TMEM68 knockout had little impact. **Conclusion** The TMEM68-mediated TAG synthesis pathway has distinct features from the canonical DGAT pathway, however, TMEM68 and DGAT may coregulate intracellular TAG levels.

Key words triacylglycerol, lipid droplet, TMEM68, DGAT

DOI: 10.16476/j.pibb.2024.0287

CSTR: 32369.14.pibb.20240287

Triacylglycerols (TAGs) are complex neutral lipids composed of a glycerol backbone linked to three fatty acyl chains^[1]. TAGs are synthesized in the endoplasmic reticulum (ER) and stored in cytosolic lipid droplets (LDs), which constitute a major cellular reservoir of energy, signaling lipids and membrane structure components^[2-3]. The main well-known pathways for TAG biosynthesis in mammals include the monoacylglycerol (MAG) and glycerol-3-phosphate (G3P) pathways^[4]. The MAG pathway operates in a restricted set of tissues, including the small intestine, adipose tissue, and liver^[5-6], whereas the G3P pathway, also known as the *de novo* synthesis pathway, contributes the majority of TAGs in most cells and tissues^[7]. These two classical TAG synthesis pathways converge in a common final step, which

acylates diacylglycerol (DAG) with fatty acyl-coenzyme A (CoA) by acyl-CoA: diacylglycerol acyltransferase (DGAT) to form TAGs^[8]. In addition, an alternative TAG biosynthesis pathway driven by transmembrane protein 68 (TMEM68), also known as DGAT1/2-independent enzyme synthesizing storage lipids (DIESL), was recently identified in mammals^[9].

Two DGAT isoenzymes, DGAT1 and DGAT2

* This work was supported by grants from Chongqing Natural Science Foundation (CSTB2022NSCQ-MSX0957) and the Science and Technology Research Program of Chongqing Municipal Education Commission (KJQN20230065).

** Corresponding author.

Tel: 86-23-62460536, E-mail: changpa@cqupt.edu.cn

Received: July 1, 2024 Accepted: October 11, 2024

can utilize *de novo* synthesized or exogenously supplied fatty acid (FA) to esterify DAG, with a preference of DGAT1 for exogenous and recycling FA, while a priority of DGAT2 to *de novo* synthesized FA^[10-12]. DGAT1 is primarily anchored on the ER membrane and is implicated in the biogenesis of new LDs^[13], whereas DGAT2 can also localize to mitochondria and LDs and may promote LD expansion^[11, 14-15]. In mammals, DGAT1 and DGAT2 account for the majority of TAG synthesis in most cell types and tissues^[11, 16-17]. However, DGAT1/2 adipose specific double-knockout mice retained a substantial amount of TAG in their adipocytes^[18], which suggested the presence of additional enzymes responsible for mammalian TAG synthesis.

One candidate enzyme recently implicated in mammalian TAG synthesis is TMEM68, a poorly characterized acyltransferase with weak sequence homology to monoacylglycerol acyltransferase (MGAT) and DGAT enzymes^[19]. TMEM68 is anchored on the ER membrane and is expressed in adult mouse brain at a higher level than other tissues^[19]. The ectopic expression of TMEM68 promotes TAG storage and LD accumulation dependently on the presence of conserved acyltransferase catalytic active sites^[20]. In addition, DGAT1 activity is not required for the increased TAG levels due to TMEM68 overexpression^[20]. TMEM68 was recently demonstrated to synthesize TAG using DAG as an acyl acceptor independent of DGAT, which was under potent control by thioredoxin-related transmembrane protein 1 (TMX1)^[9]. TMEM68 overexpression increased TAG levels and reduced contents of glycerophospholipids (GPLs), especially phosphatidylcholine (PC) and ether-linked PC^[9, 20], suggesting the potential utilization of phospholipids as an acyl donor. In contrast, our previous results showed 20%–30% reduction of TAG levels due to TMEM68 knockout (KO) or knockdown without DGAT inhibition^[21]. Thus, the TMEM68-mediated pathway accounts for a small but discrete proportion of basal cellular TAG synthesis in mammalian cells.

Compared with wild-type mice, global *Tmem68*-KO mice exhibited a lower body weight, shorter body size, less body fat and decreased plasma TAGs^[9], indicating that DGATs cannot compensate for TMEM68 deficiency. During lipids deprivation, TMEM68 is required for the production of TAG to provide FAs for mitochondrial breakdown at the

expense of membrane phospholipids^[9]. The emerging data suggest unique roles for TMEM68 and DGATs in TAG synthesis from distinct pools of FAs. Whether the alternative TAG production process affects LD formation and the interplay between TMEM68 and DGAT under different metabolic conditions or across cell types remain unclear. In the present study, the roles of TMEM68 and DGATs in TAG synthesis and LD formation and their relationships were further explored based on our previously generated TMEM68-overexpressing and TMEM68-KO human neuroblastoma cell models.

1 Materials and methods

1.1 Cell culture and transfection

SK-N-SH and HEK293 cells were cultured in DMEM supplemented with 10% fetal bovine serum (FBS), 100 U/ml penicillin and 100 mg/L streptomycin in a 37°C incubator with 5% CO₂. SK/TMEM68 cells and SK/TMEM68 KO cells stably overexpressing and knocking out TMEM68, respectively, were cultured in complete medium supplemented with 0.5 mg/L puromycin^[21]. The plasmids pTMEM68-GFP and pDGAT1-mCherry (constructed by Jiangsu GeneCfPs Biotechnology Co., Ltd., China) were co-transfected into HEK293 cells using Lipofectamine 2000 (Thermo Fisher Scientific, USA).

1.2 Oil Red O staining

Cells were treated with vehicle (0.1% DMSO), 10 μmol/L DGAT1 inhibitor T863 (MCE, Shanghai, China), 5 μmol/L DGAT2 inhibitor PF06424439 methanesulfonate (MCE, Shanghai, China) alone or both DGAT inhibitors for 6 h in the presence or absence of 0.1 mmol/L monoacylglycerol (MAG), 1-oleoyl-*rac*-glycerol (Sigma-Aldrich, Shanghai, China). For cells incubated with MAG and DGAT inhibitor together, cells were preincubated with DGAT inhibitor for 1 h. After removing the medium and washing with PBS, the cells were fixed with 4% paraformaldehyde in PBS for 10 min at room temperature and then stained using an Oil Red O (ORO) staining kit (Solarbio, Beijing, China). Cell images were acquired using an Olympus IX73 inverted microscope. The area stained with ORO was quantified using ImageJ image analysis software^[22].

1.3 Confocal fluorescence microscopy

For detection of LDs, cells were seeded in

12-well plates mounted onto cover slips. After seeding for 24 h, cells were treated with vehicle (0.1% DMSO), 10 $\mu\text{mol/L}$ T863, 5 $\mu\text{mol/L}$ PF06424439 methanesulfonate or both inhibitors for 6 h in the presence or absence of 0.2 mmol/L oleic acid (OA) complexed with fat-free BSA for 6 h. Before incubation with OA and DGAT inhibitor together, cells were treated with DGAT inhibitor for 1 h. Then cells were washed with PBS twice and fixed with 4% paraformaldehyde for 30 min at room temperature. LDs were stained with HCS LipidTOX™ Deep Red (Thermo Fisher Scientific, USA) (1:1 000 in PBS) for 30 min. After brief washes with PBS, nuclei were stained with 0.5 mg/L DAPI for 15 min. To detect colocalization of TMEM68 and DGAT1, cells were washed with PBS twice after transfection for 48 h and fixed with paraformaldehyde at room temperature. Then cells were washed briefly and nuclei were stained with DAPI. Slides were sealed with antifade mounting medium and stored at 4°C. Fluorescence images were captured with an Olympus SpinSR confocal microscope. HCS LipidTOX™ Deep Red was excited at 633 nm, and emission was detected between 650 and 700 nm. DAPI was excited at 364 nm, and emission was detected between 450 and 490 nm. GFP was excited at 488 nm, and emission was detected between 500 and 530 nm. mCherry was excited at 561 nm, and emission was detected between 580 and 610 nm. All the presented experiments were repeated independently at least 3 times. LD area (2D) was quantitatively determined using the ImageJ Auto Local Threshold tool (Bernsen method).

1.4 TAG levels assay

TAG levels were determined with an enzyme-based triglyceride assay kit (Applygen, Beijing, China). Briefly, cells were harvested and dissolved in lysis buffer (100 $\mu\text{l}/10^6$ cells). After a brief centrifugation, the protein concentration of the supernatant was measured with a BCA protein assay kit (Beyotime Biotechnology, Shanghai, China). The supernatant was then heated for 10 min at 70°C and centrifuged for 5 min at 2 000 r/min. TAG levels in the supernatant were determined according to the manual of the triglyceride assay kit.

1.5 Co-immunoprecipitation

Co-immunoprecipitation (Co-IP) was performed according to the manual of the Co-IP kit (Wuhan

Gene Create Biological Engineering Co., Ltd., China). Briefly, HEK293 cells were co-transfected with TMEM68-GFP and DGAT1-mCherry plasmid DNA. 48 h post transfection, cells (approximately 2×10^7) were solubilized with 1 ml of lysis buffer containing 1% protease inhibitor for 30 min and then sonicated. Insoluble material was removed by centrifugation at 15 000g for 10 min at 4°C, and the solubilized material was transferred to a fresh tube. A 100 μl aliquot (10% of the total) was removed to determine the protein levels (input). A 450 μl aliquot was incubated with 3–5 μg of anti-GFP or anti-mCherry antibody overnight. Control experiments were performed using normal mouse IgG (5 μg). Protein A/G magnetic beads (30 μl) were then added and rotated for 2 h. The beads were washed with wash buffer, and the bound proteins were eluted with 100 μl of elution buffer. A 30 μl aliquot of the immunoprecipitates was analyzed by immunoblotting with anti-mCherry or anti-GFP antibodies (Proteintech, Wuhan, China) (1 : 1 000 dilution). All manipulations were performed at 4°C.

1.6 RNA extraction and RT-qPCR

Total RNA was extracted using a FastPure® Cell/Tissue Total RNA Isolation Kit V2 (Vazyme Biotechnology, Nanjing, China) and then transcribed to cDNA with a HiScript III All-in-one RT SuperMix Perfect for quantitative PCR (qPCR) Kit (Vazyme Biotechnology). Real-time qPCR was performed with ChamQ SYBR qPCR Master Mix (Vazyme Biotechnology) on a Bio-Rad IQ5 qPCR System. The following primers were used: *hDGAT1* fw 5'-CGGT-CCCAATCACCTCATCTG-3'; *hDGAT1* rv 5'-TGC-ACAGGGATGTTCCAGTTC-3'; *hactin* fw 5'-CAT-GTACGTTGCTATCCAGGC-3'; and *hactin* rv 5'-CT-CCTTAATGTCACGCACGAT-3'. Relative mRNA levels were quantified according to the $\Delta\Delta C_t$ method using β -actin as a reference gene^[23].

1.7 Immunoblotting assay

Total protein extract was prepared in RIPA buffer supplemented with 1 mmol/L phenylmethanesulfonyl fluoride (PMSF) by sonication and then centrifuged at 15 000g for 15 min at 4°C to pellet the cell debris. The supernatant protein concentration was determined with a BCA protein assay kit. The supernatant was mixed with 5×SDS loading buffer and boiled for 5 min. All the samples were subjected to SDS/PAGE, transferred to nitrocellulose filters and subjected to

immunoblotting analysis using an anti-DGAT1 antibody (1 : 1 000 dilution) and an anti-GAPDH antibody (1 : 5 000 dilution) (Proteintech, Wuhan, China) as described previously^[24]. The blots were quantified by ImageJ (1.43) software.

1.8 Statistical analysis

All graphs and statistical analyses were generated using GraphPad Prism 9 (GraphPad Software, Inc., La Jolla, CA, USA). Bar graphs represent means±SD. Statistical comparisons for two groups were performed by the Student's *t* test and for more than two groups by ordinary one-way ANOVA followed by Tukey's multiple comparison testing. Group differences between means were considered significant at $P < 0.05$.

2 Results

2.1 TAG synthesis and LD formation catalyzed by TMEM68 are independent of DGAT activity

LDs are required to store TAGs. The effect of TMEM68 on LD formation is not well known. As shown in Figure 1a, a small number of LDs were present in human neuroblastoma SK-N-SH cells, and fewer and smaller-sized LDs were observed after DGAT1/2 inhibition (D1D2i). LDs content was significantly increased in SK/TMEM68 cells compared with SK-N-SH cells, but was not significantly decreased by D1D2i (Figure 1b). OA supplementation increased the size and number of LDs in SK-N-SH cells, which was significantly blocked by D1D2i (Figure 1a). Conversely, neither OA loading nor DGAT1/2 inactivation significantly altered the content of LDs in SK/TMEM68 cells (Figure 1b). TAG levels were elevated and reduced significantly by exogenous OA challenge and D1D2i in SK-N-SH cells (Figure 1c). In contrast, TAG content was not affected by OA loading in SK/TMEM68 cells or decreased due to both DGAT activities inhibition (Figure 1c). Thus, surplus exogenous FAs were channeled into TAG and stored in LDs mainly through DGAT, and TMEM68 was capable of promoting TAG and LDs formation independently of DGAT.

In addition to FAs, MAG is also utilized for TAG biosynthesis through the MAG pathway. MAG stimulation resulted in an increased number of cells stained positive for ORO and a significant increase in the staining intensity in human neuroblastoma cells

(Figure 2a). Compared with the vehicle group, the ORO staining area and TAG levels were increased more than 5-fold by MAG treatment in SK-N-SH cells (Figure 2b, c). When both DGAT activities were inhibited pharmacologically using established small molecule inhibitors, almost no ORO staining was observed in the presence of exogenous MAG. This inhibitory effect occurred mainly through DGAT1, but not DGAT2 inactivation (Figure 2), suggesting DGAT1 was the dominant enzyme for TAG synthesis using MAG in SK-N-SH cells. In contrast, ORO staining and TAG levels in SK/TMEM68 cells were insensitive to MAG treatment and DGAT1/2 inhibition (Figure 2), showing that TMEM68 was capable of promoting TAG accumulation independently of DGAT and exogenous MAG. We next repeated these experiments with TMEM68 KO cells and found that ORO staining and TAG content were increased significantly upon MAG treatment and decreased to undetectable levels by DGAT1/2 inhibitors, which was indistinguishable from the findings in SK-N-SH cells (Figure 2). This further suggested that the incorporation of exogenous MAGs strictly requires DGATs, mainly DGAT1 and TMEM68 did not efficiently metabolize exogenously provided MAGs for TAG synthesis.

2.2 TMEM68 and DGAT differentially contribute to LD formation

The contributions of DGAT and TMEM68 to LD formation were further investigated in human neuroblastoma cells. Compared with SK-N-SH cells, almost no LDs were observed in SK/TMEM68 KO cells after inhibition of DGAT1/2 (Figure 3a, b), showing that TMEM68 and DGAT1/2 contributed to LD formation. In SK-N-SH cells treated with DGAT1/2 inhibitors, the content of LDs was significantly reduced and only few LDs with larger size were present, suggesting TMEM68 may contribute to the formation of large LDs. This was further supported by the presence of medium- and small-sized LDs in SK/TMEM68 KO cells without DGAT1/2 inhibitors. The contribution of DGAT1 and DGAT2 alone to LDs formation was further explored in TMEM68 deficiency cells. DGAT1 inhibitor (D1i) led to the disappearance of almost all but a few small-sized LDs and a significant reduction in LDs content in SK/TMEM68 KO cells, whereas DGAT2 inhibitor (D2i) had little effect on LD formation (Figure 3),

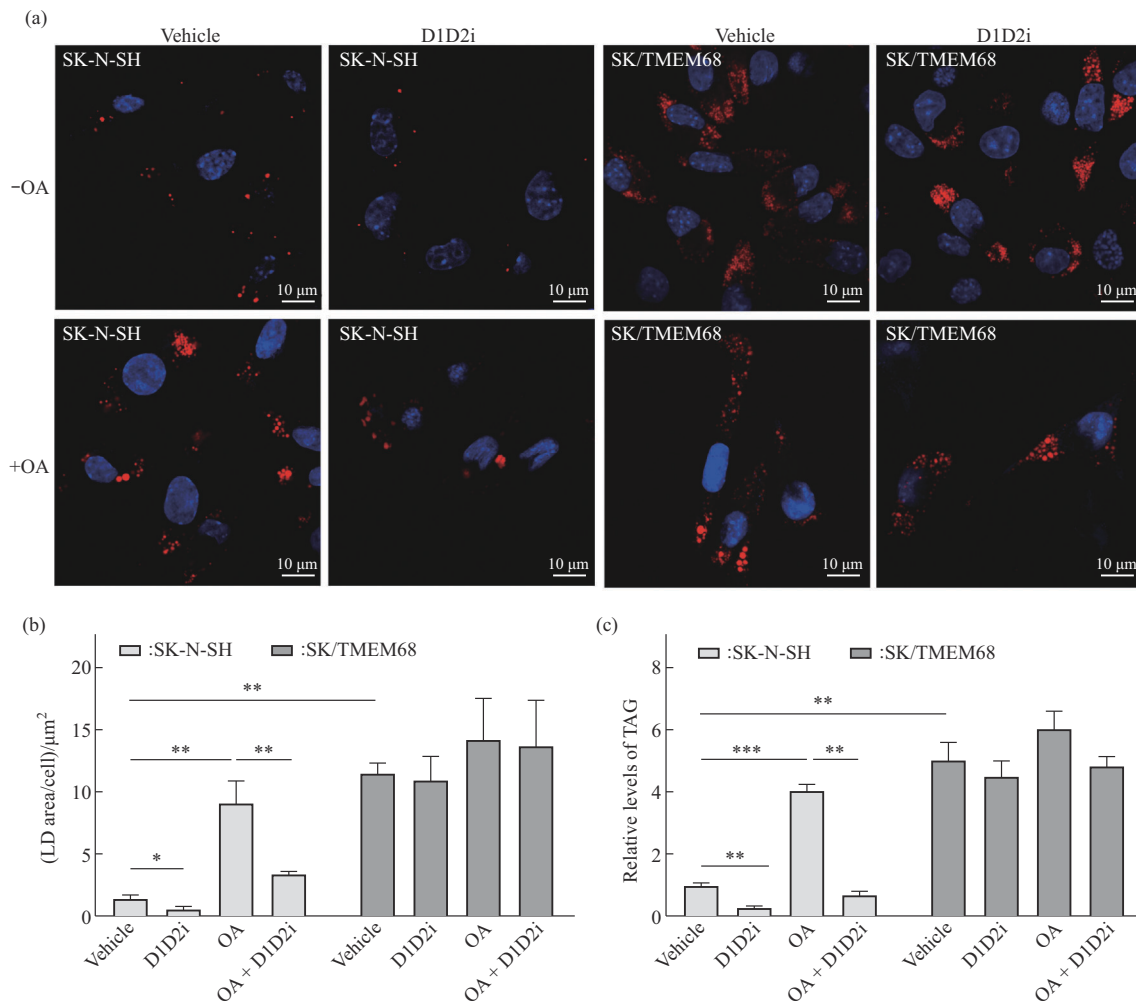


Fig. 1 LD and TAG formation driven by TMEM68 was independent of DGAT activity

(a) SK-N-SH and SK/TMEM68 (TMEM68-overexpressing) cells were cultured in medium supplemented with OA (+OA) or not (-OA) and treated with DGAT1/2 inhibitors together (D1D2i) or vehicle for 6 h. Cells were preincubated with D1D2i for 1 h before OA loading. LDs and nuclei were visualized using HSC LipidTOX Deep Red and DAPI, respectively. Images were acquired by confocal fluorescence microscopy. (b) LD area/cell in (a) was quantified using the ImageJ from 5 images for each treatment. Data were from a representative experiment that was repeated twice. (c) TAG levels were determined in 3 independent samples. Data are representative of three independent experiments and are presented as mean±SD. * $P < 0.05$, ** $P < 0.01$, *** $P < 0.001$.

showing that DGAT1 functions as the major DGAT enzyme responsible for LDs formation. Collectively, TMEM68 and DGAT1/2 have distinct contributions to LD biogenesis.

2.3 TMEM68 colocalizes but does not interact with DGAT1

TMEM68 and DGAT1 are the ER-anchored membrane proteins that contribute to TAG synthesis^[13, 19], but how do they coordinately synthesize TAG? We first co-expressed TMEM68 and DGAT1 and observed their subcellular localization in HEK293 cells. As shown in Figure 4, ectopically

expressed GFP alone was diffusely distributed throughout the cell, whereas TMEM68 fused with GFP (TMEM68-GFP) exhibited a reticulate pattern in the cytoplasm. Similarly, DGAT1 tagged with mCherry (DGAT1-mCherry) also displayed a reticulate pattern. Thus, GFP overlapped with DGAT1 to a minimal extent, whereas TMEM68 and DGAT1 completely overlapped with each other in terms of subcellular localization, revealing the colocalization of both TMEM68 and DGAT1 in the ER. Next, we performed co-IP experiments to investigate the interaction of TMEM68 and DGAT1. The co-expression of TMEM68-GFP and DGAT1-mCherry

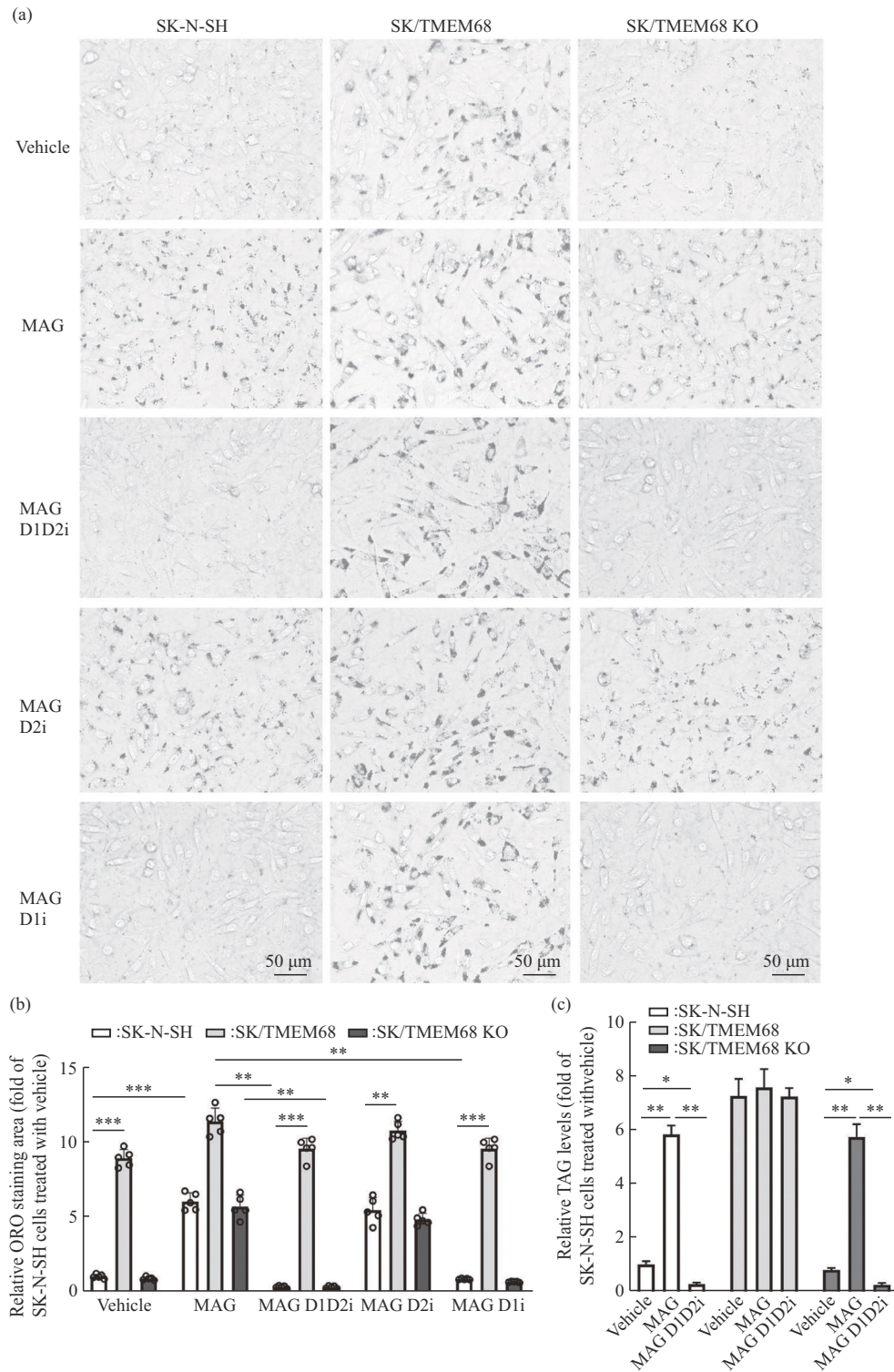


Fig. 2 The synthesis of TAG catalyzed by TMEM68 was not altered by exogenous MAG

(a) Accumulation of TAG as assessed by ORO staining. SK-N-SH, SK/TMEM68 (TMEM68-overexpressing) and SK/TMEM68 KO (TMEM68 knockout) cells were preincubated for 1 h with DGAT1 inhibitor (D1i), DGAT2 inhibitor (D2i) alone or DGAT1/2 inhibitors together (D1D2i) followed by incubation with 0.1 mmol/L MAG or vehicle in the presence/absence of DGAT inhibitors for 6 h. Cells were fixed and then stained with ORO. Images were acquired to visualize TAGs. Three images were randomly acquired in each well. (b) Quantification of ORO staining area in (a) by the ImageJ. Total LD area of 3 random images per well was quantified and 5 wells were counted for every sample. Data are from a representative experiment that was repeated twice. (c) TAG levels measurement in (a), $n=3$. Data are presented as mean \pm SD. * $P<0.05$, ** $P<0.01$, *** $P<0.001$.

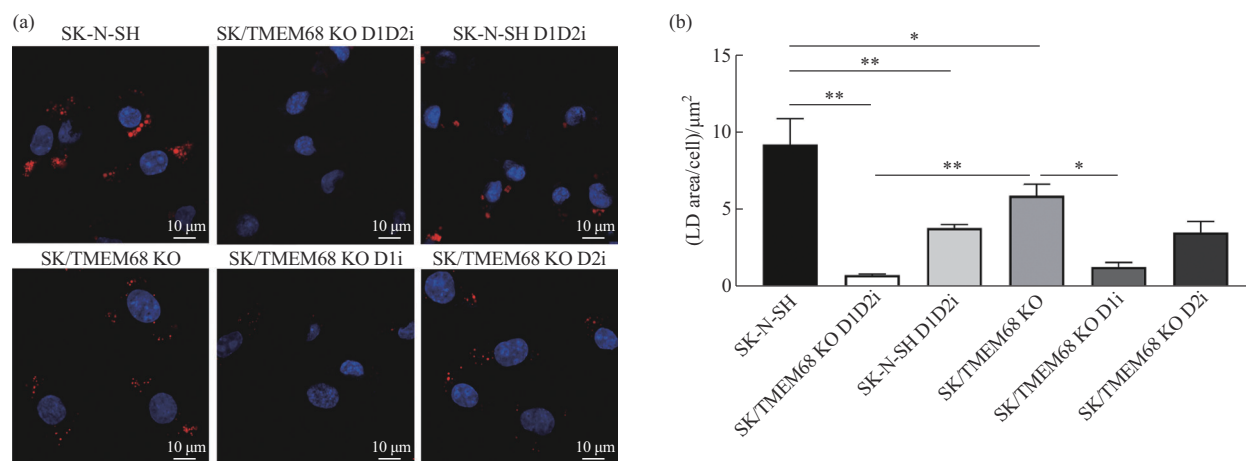


Fig. 3 Contribution of TMEM68 and DGAT to LD formation in mammalian cells

(a) SK-N-SH and SK/TMEM68 KO (TMEM68 knockout) cells were preincubated for 1 h with DGAT1 inhibitor (D1i), DGAT2 (D2i) alone, in combination or not, followed by incubation with OA±DGAT inhibitor for 6 h. LDs and nuclei were visualized using HSC LipidTOX Deep Red and DAPI, respectively. Images were acquired by confocal fluorescence microscopy. (b) Quantification of LD area in (a). LD area/cell in 5 images for each sample was quantified. Data are from a representative experiment that was repeated twice and are presented as mean±SD. * $P < 0.05$, ** $P < 0.01$.

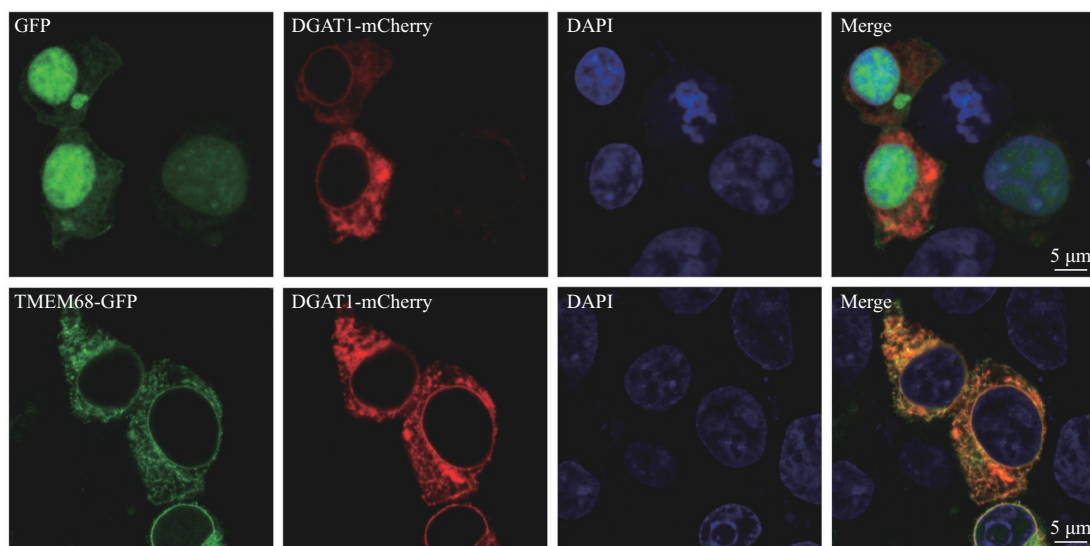


Fig. 4 Colocalization of DGAT1 and TMEM68 in mammalian cells

GFP or TMEM68-GFP and DGAT1-mCherry were co-expressed in HEK293 cells, and their subcellular distribution was observed by confocal fluorescence microscopy. Nuclei were visualized with DAPI. The images were representative results from 3 independent experiments.

was confirmed by immunoblotting lysates of transfected cells with anti-GFP and anti-mCherry antibodies (Figure 5, Input). TMEM68-GFP was immunoprecipitated using an anti-GFP antibody with normal IgG as a control. No immunoreactive material was observed when anti-GFP immunoprecipitates were immunoblotted with anti-mCherry, similar to the normal IgG control, whereas DGAT1-mCherry was

detected in the supernatant (Figure 5a). The expression of GAPDH was detected only in the supernatant and input. Similar results were observed when anti-mCherry and anti-GFP antibodies were used for IP and WB, respectively (Figure 5b). These results together showed that TMEM68 does not interact with DGAT1.

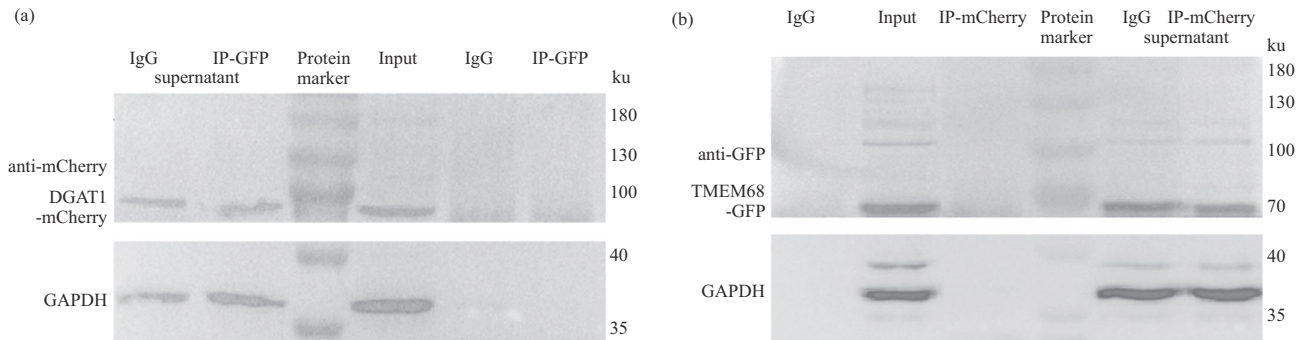


Fig. 5 Co-IP of TMEM68 and DGAT1 from HEK293 cells

TMEM68-GFP was co-expressed with DGAT1-mCherry. (a) DGAT1 was immunoprecipitated with an anti-GFP antibody, and normal IgG was used as the control. Input, IP and IP supernatants were separated by SDS-PAGE and then probed with anti-mCherry. (b) TMEM68 was immunoprecipitated with an anti-mCherry antibody, and normal IgG was used as the control. Input, IP and IP supernatants were separated by SDS-PAGE and then probed with anti-GFP. GAPDH was used as a protein loading control. The blots were representative results from 3 independent experiments.

2.4 TMEM68 influences the expression of DGAT1

Although TMEM68 does not interact with DGAT1, whether TMEM68 influences DGAT1 expression to coordinate intracellular TAG synthesis is unclear. In human neuroblastoma cells, TMEM68 overexpression significantly reduced the mRNA

levels of *DGAT1* gene by about 0.4-fold of control cells, while TMEM68 deficiency had little effect (Figure 6a). These findings were further confirmed at the protein level. As shown in Figure 6b, TMEM68 overexpression downregulated the expression of DGAT1 by approximate 35%, whereas TMEM68 KO did not affect DGAT1 levels compared with SK-N-SH control cells.

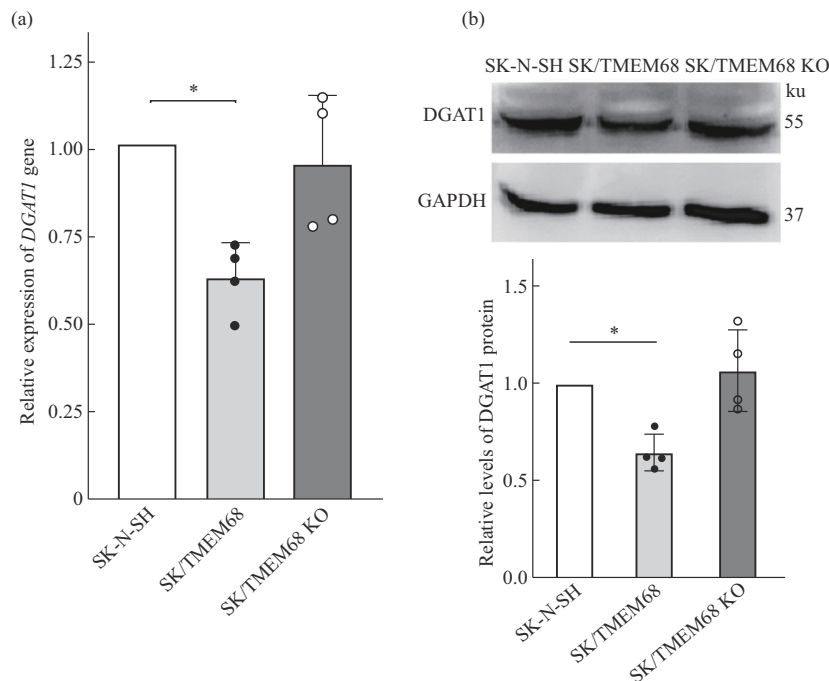


Fig. 6 TMEM68 affected the expression of DGAT1 in human neuroblastoma cells.

(a) mRNA levels of *DGAT1* gene were quantified by qPCR. (b) The expression of DGAT1 was detected by Western blot and quantified. The expression of GAPDH was used as an internal control. Data are presented as mean±SD. **P*<0.05, *n*=4.

3 Discussion

TAG synthesis is tightly and accurately regulated in the body. To date, the canonical TAG synthesis pathway carried out by DGAT and an alternative pathway catalyzed by TMEM68 have been identified in mammals^[1, 8-9]. DGATs utilize FA to esterify DAG with a preference of DGAT1 for exogenous and recycling FA, as well as DGAT2 for *de novo* synthesized FA^[10-12]. In human neuroblastoma cells, DGAT1 was demonstrated to be the dominant enzyme utilizing exogenously supplied surplus FA and MAG to synthesize TAG and form LDs. TMX1 usually restricts TMEM68-catalyzed TAG synthesis^[9]. Overexpression of TMEM68 still promotes TAG and LDs accumulation independent of DGAT in the presence of TMX1. TMEM68 may not be able to efficiently utilize excess exogenous OA and MAG for TAG synthesis

TAGs synthesized by both DGAT1 and DGAT2 affect the size and number of LDs in primary hepatocytes^[11], human hepatocellular carcinoma cells^[12, 25], adipocytes^[13] and human skeletal muscle cells^[26]. Here, TMEM68 and DGAT1/2 were found to be responsible for LD formation in human neuroblastoma cells. TAG synthesis and LD formation were mainly dependent on DGATs, especially DGAT1, and TAGs synthesized by TMEM68 were stored in a few large LDs. Conversely, TAGs synthesized through the canonical DGAT-dependent pathway led to more and smaller-sized LDs formation. The distinct sizes and numbers of LDs formed by TMEM68 and DGATs may be related to TAG composition for their differential access to precursor pools. Both DGAT1 and DGAT2 catalyze the transfer of a fatty acyl group from FA-derived fatty acyl-CoA to DAG, thereby forming TAG^[10-12], while TMEM68 possibly transfers fatty acyl groups from membrane GPLs to DAG^[9]. TMEM68 deficiency led to a biased depletion of highly unsaturated TAG species^[21], suggesting that endogenous TMEM68 preferentially (may not exclusively) incorporates polyunsaturated fatty acyl form GPLs into DAG. In addition to TAG synthesis, TMEM68 appears to have a function in basal cellular GPLs remodeling and PUFAs homeostasis^[21]. GPLs metabolism has been linked to LD formation^[27-28]. How the alternative TAG biosynthesis pathway driven

by TMEM68 affects LD biogenesis needs to be further revealed at the molecular level. In addition, LD size and TAG components are crucial for determining the catabolism of LDs and the ultimate fate of the released FAs^[25, 29]. Thus, it will be necessary to elucidate the catabolism of LDs formed by TMEM68 and the utilization of FAs released under different metabolic conditions and across cell types.

DGAT1 and TMEM68 are integral membrane proteins in the ER^[13, 19]. DGAT1 is the major enzyme responsible for TAG synthesis and TMEM68 synthesized TAG independent of DGAT in human neuroblastoma cells. Plants, yeast and microalgae employ a well-known acyl-CoA independent pathway for TAG synthesis, in which a fatty acyl is transferred from GPLs to DAG *via* the enzyme phospholipid: diacylglycerol acyltransferase (PDAT)^[30-31]. In *Arabidopsis*, PDAT1 interacts with DGAT1 to enhance TAG assembly^[32]. Although TMEM68 colocalized with DGAT1 in the same subcellular compartment, they did not interact each other in mammalian cells. Overexpression of TMEM68 reduced the expression of DGAT1, resulting in a non-significant change LDs content in response to medium supplemented with exogenously OA or MAG. This may be an adaptive mechanism of TMEM68 overexpression leading to an increase in TAG content. In contrast, TMEM68 deficiency did not affect the expression of DGAT1, which may be owing to a less reduction in TAG levels (approximate 30%)^[21]. However, TMEM68 is widely expressed in human organs, indicating that it may play a role in maintaining lipid homeostasis beyond TAG in multiple tissues.

4 Conclusion

Taking together, our findings demonstrate that TMEM68 and DGAT1 colocalize to the same ER subdomain to coordinate TAG synthesis by regulating gene expression without interaction. TMEM68 may have different precursor pools from DGAT to synthesize TAG in a DGAT-independent manner, leading to LDs with unique characteristics compared to those formed by DGAT.

Acknowledgments We thank WANG Shi-Chun and ZHENG Wen-Xia (Southwest Hospital, Army Medical University) for their assistance with confocal fluorescence microscopy.

References

- [1] Schaffer J E. Previously unknown pathway for lipid biosynthesis discovered. *Nature*, 2023, **621**(7977): 47-48
- [2] Zadoorian A, Du X, Yang H. Lipid droplet biogenesis and functions in health and disease. *Nat Rev Endocrinol*, 2023, **19**: 443-459
- [3] Walther T C, Chung J, Farese RV. Lipid droplet biogenesis. *Annu Rev Cell Dev Biol*, 2017, **33**: 491-510
- [4] Coleman R A, Mashek D G. Mammalian triacylglycerol metabolism: synthesis, lipolysis, and signaling. *Chem Rev*, 2011, **111**(10): 6359-6386
- [5] Yen C L E, Nelson D W, Yen M I. Intestinal triacylglycerol synthesis in fat absorption and systemic energy metabolism. *J Lipid Res*, 2015, **56**(3): 489-501
- [6] Stone S J. Mechanisms of intestinal triacylglycerol synthesis. *Biochim Biophys Acta Mol Cell Biol Lipids*, 2022, **1867**(6): 159151
- [7] Wang H, Airola M V, Reue K. How lipid droplets “TAG” along: glycerolipid synthetic enzymes and lipid storage. *Biochim Biophys Acta Mol Cell Biol Lipids*, 2017, **1862**(10 Pt B): 1131-1145
- [8] Chen G, Harwood J L, Lemieux M J, *et al.* Acyl-CoA: diacylglycerol acyltransferase: properties, physiological roles, metabolic engineering and intentional control. *Prog Lipid Res*, 2022, **88**: 101181
- [9] McLelland G L, Lopez-Osias M, Verzijl C R C, *et al.* Identification of an alternative triglyceride biosynthesis pathway. *Nature*, 2023, **621**(7977): 171-178
- [10] Villanueva C J, Monetti M, Shih M, *et al.* Specific role for acyl CoA: diacylglycerol acyltransferase 1 (Dgat1) in hepatic steatosis due to exogenous fatty acids. *Hepatology*, 2009, **50**(2): 434-442
- [11] Li C, Li L, Lian J, *et al.* Roles of acyl-CoA: diacylglycerol acyltransferases 1 and 2 in triacylglycerol synthesis and secretion in primary hepatocytes. *Arterioscler Thromb Vasc Biol*, 2015, **35**(5): 1080-1091
- [12] Wurie H R, Buckett L, Zammit V A. Diacylglycerol acyltransferase 2 acts upstream of diacylglycerol acyltransferase 1 and utilizes nascent diglycerides and *de novo* synthesized fatty acids in HepG2 cells. *FEBS J*, 2012, **279**(17): 3033-3047
- [13] Chitraju C, Mejhert N, Haas J T, *et al.* Triglyceride synthesis by DGAT1 protects adipocytes from lipid-induced ER stress during lipolysis. *Cell Metab*, 2017, **26**(2): 407-418.e3
- [14] Stone S J, Levin M C, Zhou P, *et al.* The endoplasmic reticulum enzyme DGAT2 is found in mitochondria-associated membranes and has a mitochondrial targeting signal that promotes its association with mitochondria. *J Biol Chem*, 2009, **284**(8): 5352-5361
- [15] McFie P J, Banman S L, Stone S J. Diacylglycerol acyltransferase-2 contains a c-terminal sequence that interacts with lipid droplets. *Biochim Biophys Acta Mol Cell Biol Lipids*, 2018, **1863**(9): 1068-1081
- [16] Harris C A, Haas J T, Streeper R S, *et al.* DGAT enzymes are required for triacylglycerol synthesis and lipid droplets in adipocytes. *J Lipid Res*, 2011, **52**(4): 657-667
- [17] Roe N D, Handzlik M K, Li T, *et al.* The role of diacylglycerol acyltransferase (DGAT) 1 and 2 in cardiac metabolism and function. *Sci Rep*, 2018, **8**: 4983
- [18] Chitraju C, Fischer A W, Ambaw Y A, *et al.* Mice lacking triglyceride synthesis enzymes in adipose tissue are resistant to diet-induced obesity. *Elife*, 2023, **12**: RP88049
- [19] Chang P A, Heier C, Qin W, *et al.* Molecular identification of transmembrane protein 68 as an endoplasmic reticulum-anchored and brain-specific protein. *PLoS One*, 2017, **12**(5): e0176980
- [20] Wang Y, Zeng F, Zhao Z, *et al.* Transmembrane protein 68 functions as an MGAT and DGAT enzyme for triacylglycerol biosynthesis. *Int J Mol Sci*, 2023, **24**(3): 2012
- [21] Zeng F, Heier C, Yu Q, *et al.* Human transmembrane protein 68 links triacylglycerol synthesis to membrane lipid homeostasis. *bioRxiv*, 2024. doi:10.1101/2024.04.14.589399
- [22] Jin Y, McFie P J, Banman S L, *et al.* Diacylglycerol acyltransferase-2 (DGAT2) and monoacylglycerol acyltransferase-2 (MGAT2) interact to promote triacylglycerol synthesis. *J Biol Chem*, 2014, **289**(41): 28237-28248
- [23] Schmittgen T D, Livak K J. Analyzing real-time PCR data by the comparative C(T) method. *Nat Protoc*, 2008, **3**(6): 1101-1108
- [24] Heier C, Kien B, Huang F, *et al.* The phospholipase PNPLA7 functions as a lysophosphatidylcholine hydrolase and interacts with lipid droplets through its catalytic domain. *J Biol Chem*, 2017, **292**(46): 19087-19098
- [25] Selvaraj R, Zehnder S V, Watts R, *et al.* Preferential lipolysis of DGAT1 over DGAT2 generated triacylglycerol in Huh7 hepatocytes. *Biochim Biophys Acta Mol Cell Biol Lipids*, 2023, **1868**(10): 159376
- [26] Løvstetten N G, Vu H, Skagen C, *et al.* Treatment of human skeletal muscle cells with inhibitors of diacylglycerol acyltransferases 1 and 2 to explore isozyme-specific roles on lipid metabolism. *Sci Rep*, 2020, **10**(1): 238
- [27] Farese R V, Walther T C. Glycerolipid synthesis and lipid droplet formation in the endoplasmic reticulum. *Cold Spring Harb Perspect Biol*, 2023, **15**(5): a041246
- [28] Penno A, Hackenbroich G, Thiele C. Phospholipids and lipid droplets. *Biochim Biophys Acta*, 2013, **1831**(3): 589-594
- [29] Schott M B, Weller S G, Schulze R J, *et al.* Lipid droplet size directs lipolysis and lipophagy catabolism in hepatocytes. *J Cell Biol*, 2019, **218**(10): 3320-3335
- [30] Sah S K, Fan J, Blanford J, *et al.* Physiological functions of phospholipid: diacylglycerol acyltransferases. *Plant Cell Physiol*, 2024, **65**(6): 863-871
- [31] Barbosa A D, Siniouoglou S. Membranes that make fat: roles of membrane lipids as acyl donors for triglyceride synthesis and organelle function. *FEBS Lett*, 2024, **598**(10): 1226-1234
- [32] Lee H G, Seo P J. Interaction of DGAT1 and PDAT1 to enhance TAG assembly in *Arabidopsis*. *Plant Signal Behav*, 2019, **14**(1): 1554467

跨膜蛋白68和二酰甘油酰基转移酶在脂肪合成和脂滴形成中的不同作用*

余庆 付洋洋 曾繁思 逢慧敏 黄飞飞 常平安**

(重庆邮电大学生命健康信息科学与工程学院, 重庆市大数据生物智能重点实验室, 重庆 400065)

摘要 **目的** 表征一条三酰甘油 (TAG) 生物合成替代途径中的跨膜蛋白 68 (TMEM68), 并确定 TMEM68 与经典 TAG 合成酶酰基辅酶 A: 二酰甘油酰基转移酶 (DGAT) 之间的相互作用。**方法** 通过比较 DGAT 抑制剂处理与否的脂滴形态、油红 O 染色面积以及 TAG 水平, 研究外源脂肪酸和单酰甘油对 TMEM68 过表达和敲除细胞的 TAG 合成和脂滴形成的影响。脂滴采用荧光染料染色并使用共聚焦荧光显微术观察。TAG 水平使用基于酶法的脂肪检测试剂盒测定。TMEM68 和 DGAT1 的共定位通过共表达和共聚焦荧光显微术检测, 并采用免疫共沉淀检测它们的相互作用。采用逆转录定量聚合酶链反应和免疫印迹法检测 DGAT1 的表达。**结果** TMEM68 催化的 TAG 合成不依赖 DGAT 活性。在人神经母细胞瘤细胞中, 外源脂肪酸和单酰基甘油主要通过 DGAT 促进 TAG 合成。TMEM68 与 DGAT 形成的脂滴具有不同的形态。此外, TMEM68 和 DGAT1 在同一内质网 (ER) 区室共定位, 但不发生物理相互作用。TMEM68 的过表达降低了参与 TAG 合成的主要 DGAT 酶 DGAT1 的表达, 然而 TMEM68 敲除没有影响。**结论** TMEM68 介导的 TAG 合成途径具有不同于经典 DGAT 通路的特征, 然而 TMEM68 和 DGAT 可能共同调控细胞内 TAG 水平。

关键词 三酰甘油, 脂滴, 跨膜蛋白68, 二酰甘油酰基转移酶

中图分类号 Q26, Q555, Q591.5

DOI: 10.16476/j.pibb.2024.0287

CSTR: 32369.14.pibb.20240287

* 重庆市自然科学基金 (CSTB2022NSCQ-MSX0957) 和重庆市教委科技研究项目 (KJQN20230065) 资助。

** 通讯联系人。

Tel: 023-62460536, E-mail: changpa@cqupt.edu.cn

收稿日期: 2024-07-01, 接受日期: 2024-10-11